Published in final edited form as:
Exp Neurol. 2011 June ; 229(2): 409–420. doi:10.1016/j.expneurol.2011.03.008.

A selective role for ARMS/Kidins220 scaffold protein in spatial memory and trophic support of entorhinal and frontal cortical neurons

Aine M. Duffy[a,*], **Michael J. Schaner**[a], **Synphen H. Wu**[b], **Agnieszka Staniszewski**[f], **Asok Kumar**[a], **Juan Carlos Arévalo**[g], **Ottavio Arancio**[f], **Moses V. Chao**[b], and **Helen E. Scharfman**[a,c,d,e]

[a] The Nathan Kline Institute for Psychiatric Research, Center for Dementia Research, Orangeburg, New York, NY 10962, USA

[b] Molecular Neurobiology Program, Skirball Institute of Biomolecular Medicine, Departments of Cell Biology, Physiology & Neuroscience and Psychiatry, New York University Langone Medical Center, New York, NY 10016, USA

[c] Department of Child & Adolescent Psychiatry, New York University Langone Medical Center, New York, NY 10016, USA

[d] Department of Psychiatry, New York University Langone Medical Center, New York, NY 10016, USA

[e] Department of Physiology & Neuroscience, New York University Langone Medical Center, New York, NY 10016, USA

[f] Department of Pathology & Cell Biology and Taub Institute for Research on Alzheimer's Disease & the Aging Brain, Columbia University Medical Center New York, NY 10032, USA

[g] Department of Cell Biology and Pathology, Instituto de Neurociencias Castilla y Léon (INCyL), Universidad de Salamanca, Salamanca 37007, Spain

Abstract

Progressive cortical pathology is common to several neurodegenerative and psychiatric disorders. The entorhinal cortex (EC) and frontal cortex (FC) are particularly vulnerable, and neurotrophins have been implicated because they appear to be protective. A downstream signal transducer of neurotrophins, the ankyrin repeat-rich membrane spanning scaffold protein/Kidins 220 (ARMS) is expressed in the cortex, where it could play an important role in trophic support. To test this hypothesis, we evaluated mice with a heterozygous deletion of ARMS ($ARMS^{+/-}$ mice). Remarkably, the EC and FC were the regions that demonstrated the greatest defects. Many EC and FC neurons became pyknotic in $ARMS^{+/-}$ mice, so that large areas of the EC and FC were affected by 12 months of age. Areas with pyknosis in the EC and FC of $ARMS^{+/-}$ mice were also characterized by a loss of immunoreactivity to a neuronal antigen, NeuN, which has been reported after insult or injury to cortical neurons. Electron microscopy showed that there were defects in mitochondria, myelination, and multilamellar bodies in the EC and FC of $ARMS^{+/-}$ mice. Although primarily restricted to the EC and FC, pathology appeared to be sufficient to cause functional impairments, because $ARMS^{+/-}$ mice performed worse than wild-type on the Morris water maze. Comparisons of males and females showed that female mice were the affected sex in

[*]Corresponding author at: The Nathan Kline Institute for Psychiatric Research, Center for Dementia Research, 140 Old Orangeburg Rd., Bldg. 35, Orangeburg, New York, NY 10962, USA. aduffy@nki.rfmh.org (A.M. Duffy), hscharfman@nki.rfmh.org (H.E. Scharfman).

all comparisons. Taken together, the results suggest that the expression of a prominent neurotrophin receptor substrate normally protects the EC and FC, and that ARMS may be particularly important in females.

Keywords

BDNF; Neurotrophin; Sex differences; Spatial memory; Myelin; Oxidative stress

Introduction

Neurons in the entorhinal cortex (EC) and frontal cortex (FC) are vulnerable in many neurological and psychiatric disorders. Abnormal cytoarchitecture and neuron density have been observed in the EC of patients with schizophrenia (Arnold et al., 1995; Krimer et al., 1997; Arnold, 2000), temporal lobe epilepsy (Du et al., 1993; Scharfman, 2000), Alzheimer's disease (AD) and even in normal aging (Gomez-Isla et al., 1996; de Toledo-Morrell et al., 2000; Kordower et al., 2001). In the FC, it has been reported that pyramidal neurons show signs of atrophy in patients with schizophrenia (Lewis et al., 2003), bipolar disorder (Rajkowska, 2002), depression (Drevets, 2000; Shah et al., 2002), aging and AD (Holland et al., 2009; McDonald et al., 2009; Schroeter et al., 2009).

Neurotrophins may normally protect the EC and FC, because reduced expression of neurotrophins or altered neurotrophin receptors have been identified in the EC and FC in several diseases. For example, decreased levels of brain-derived neurotrophic factor (BDNF) and neurotrophin-3 (NT-3) have been found in the FC of patients with schizophrenia and drug-resistant depression (Durany et al., 2001; Weickert et al., 2003; Shoval and Weizman, 2005; Weickert et al., 2005). In addition, BDNF and its primary receptor, tropomyosin receptor kinase B (TrkB), are decreased in the cortex during aging and AD, based on both animal models of the disease, and clinical research (Lindvall et al., 1994; Knusel and Gao, 1996; Chao et al., 2006; Tapia-Arancibia et al., 2008; Nagahara et al., 2009; Peng et al., 2009).

The reasons why neurotrophins are protective in the EC and FC are unclear. Newly described signaling mechanisms suggest reasons why neurotrophins are protective, because the new pathways appear to mediate protection. One example is tyrosine phosphorylation of the ankyrin repeat-rich membrane spanning protein (ARMS), also termed Kidins220 (Iglesias et al., 2000). ARMS/Kidins220 (hereafter referred to as ARMS) is a transmembrane scaffold protein downstream of Trk (Kong et al., 2001). ARMS also is downstream of ephrin receptors, and therefore may transmit signals involved in ephrin function, such as changes in morphology and synaptic plasticity (Murai and Pasquale, 2004; Lai and Ip, 2009).

Phosphorylation of ARMS promotes cell survival in culture by activating the mitogen-activated protein kinase (MAPK) and nuclear factor κB (NFκB) (Arévalo et al., 2004, 2006; Sniderhan et al., 2008). Knockdown of ARMS in culture results in increased neuronal death (Lopez-Menendez et al., 2009), suggesting that ARMS is a candidate mechanism linking neurotrophins, and possibly ephrins, to the support of cortical neurons. Therefore, we hypothesized that decreasing levels of ARMS would result in cortical pathology. To test this hypothesis we used transgenic mice with reduced ARMS expression (heterozygous mice; $ARMS^{+/-}$). Histochemistry, immunocytochemistry, and electron microscopy (EM) were used to evaluate the EC and FC, as well as other cortical areas. The Morris water maze was used to evaluate animals behaviorally because the EC and FC have been shown to contribute to this task (Kolb et al., 1983; Hebert and Dash, 2002; Spowart-Manning and van der Staay,

2005; Nakazawa, 2006; Jo et al., 2007; Leon et al., 2010). The results suggest that ARMS plays a critical role in the maintenance of structure in the EC and FC, behaviors associated with these areas, and that sex is an important variable in the vulnerability of these regions to decreased levels of ARMS.

Materials and methods

Animals

The experimental procedures were carried out in accordance with *NIH guidelines*, and were approved by the Institutional Animal Care and Use Committees (IACUC) at The Nathan Kline Institute and New York University (NYU) Langone Medical Center. All wild-type (WT) and ARMS$^{+/-}$ mice were bred at NYU. The targeting construct for ARMS$^{-/-}$ mice has been described elsewhere (Wu et al., 2009).

Mice were housed 3–4/cage, in standard mouse cages with corn cob bedding and a 12-hour light–dark cycle (lights on, 7:00 am). Food (Purina 5001 chow; W.F. Fisher, Somerville, NJ, U.S.A.) and water were available *ad libitum*. For anatomical studies, females were perfused at the same time of day (9:00–11:00 am) and on the same stage of the estrous cycle (metestrus), to minimize variability. For the Morris water maze, the cycle stage was monitored to ensure estrous cyclicity was maintained for the duration of the testing period. To promote estrous cyclicity, males were housed in cages next to females (Whitten et al., 1968). Procedures used to establish cycle stage by vaginal cytology are described elsewhere (Scharfman et al., 2003, 2009).

Fixation and tissue preparation

WT and ARMS$^{+/-}$ mice were deeply anesthetized by inhalation (Isoflurane; Baxter Healthcare Corporation, Deerfield, IL, U.S.A.) followed by urethane (2.5 g/kg i.p.; Sigma-Aldrich Chemical Co., St. Louis, MI, U.S.A.; all chemicals were from Sigma-Aldrich unless stated otherwise), prior to fixation by perfusion through the left ventricle using a peristaltic pump (Minipuls 1, Gilson, Middleton, WI, U.S.A). This approach allowed rapid (<5 min) and sequential delivery of two solutions: normal saline (40 ml of 0.9% NaCl in distilled water; dH_2O), and fixative (40 ml of 4% paraformaldehyde in 0.1 M phosphate buffer; PB; pH 7.4). Animals used for EM were perfused with 0.9% NaCl, followed by 2% paraformaldehyde and 2.5% glutaraldehyde (Electron Microscopy Sciences, Hartfield, PA, U.S.A.) in 0.1 M PB. The brains were removed immediately, post-fixed for 24 h in 4% paraformaldehyde in 0.1 M phosphate PB at 4 °C, and horizontal sections (50 μm-thick) were cut using a vibratome (TPI 3000, Vibratome Co., St. Louis, MO, U.S.A.), and collected sequentially. Regions specified in the Results follow standard terminology (Paxinos and Franklin, 2001).

Cresyl violet stain

After the entire brain was sectioned, sections (150 μm apart) were mounted sequentially on subbed slides. After allowing slides to dry overnight, slides were dehydrated in a graded series of ethanols (Pharmaco-Aaper) diluted in distilled H_2O (dH_2O; 70%, 1×3 min; 95%, 1×3 min; and 100%, 2×5 min). Following rehydration, slides were stained with 0.1% (w/v) cresyl violet in dH_2O for 1 min. Acetic acid (0.01%; Fisher Chemical Co., Fairlawn, NJ, U.S.A.) was used to destain if sections were too dark (i.e., cells were stained, but so were areas between cells). Following dehydration, slides were cleared in xylene (2×5 min; Fisher), and cover-slipped in Permount (Fisher).

NeuN immunohistochemistry

A monoclonal antibody against neuronal nuclei (NeuN; Clone A60, MAB 377, Chemicon, Temecula, CA, U.S.A.) was purified from mouse brain, and its specificity for mature neurons has been demonstrated (Mullen et al., 1992). Notably, several recent studies have identified that neurons are not always immunoreactive using the NeuN antibody if they are evaluated after insult or injury, when NeuN is phosphorylated (Lind et al., 2005). Examples of conditions that lead to a loss of NeuN-immunoreactivity (NeuN-ir) include metabolic or oxidative stress, such as ischemia, aging, irradiation, and organophosphate toxicity (Portiansky et al., 2006; Buckingham et al., 2008; Hayakawa et al., 2008; Kadriu et al., 2009; Matsuda et al., 2009; Won et al., 2009).

Sections were chosen for NeuN-immunohistochemistry were adjacent to those that were used for cresyl violet. Sections were processed for NeuN-immunohistochemistry as previously published (Scharfman et al., 2002; Winawer et al., 2007), analyzed using a brightfield microscope (BX61, Olympus, Center Valley, PA, U.S.A.), and photographed using a digital camera (RET 2000R-F-CLR-12, Q Imaging, Surrey, BC, Canada). Some NeuN-labeled sections were counterstained with cresyl violet. For counterstaining, sections were first processed with the antibody to NeuN and then mounted on subbed slides. They were allowed to dry overnight, and then stained for cresyl violet using the protocol described above.

Image analysis (Bioquant Image Analysis Corporation, Nashville, TN, U.S.A.) was conducted as follows: first, the edges of each section were demarcated at 2× magnification. The areas displaying weak cortical NeuN-ir were then evaluated by computerized thresholding. The threshold was set so that areas such as white matter, almost exclusively without neuronal nuclei, were below threshold, and regions that had many neuronal nuclei were above the threshold. A complete 3-D rendering of each brain was compiled based on the z-coordinates for each section. Using a surface-rendering tool (Topographer Plug-in, Bioquant Image Analysis Corporation) a virtual skin was rendered using a mesh modeling algorithm for the whole brain and each region with weak NeuN-ir. This procedure led to a 3-D quantitative image of the brain (see Fig. 3), from which volumes of areas with weak NeuN were calculated.

Electron microscopy

Using tissue from animals that were fixed with paraformaldehyde/glutaraldehyde (described above), sections were processed for NeuN immunoperoxidase labeling, and adjacent sections were postfixed in 2% osmium tetroxide in 0.1 M PB for 1 h. They were processed for EM analysis as previously described (Duffy et al., 2009). Ultrathin sections were collected on 300-mesh copper grids, counterstained with 0.5% uranyl acetate (Electron Microscopy Sciences) and lead citrate (1.33 g lead nitrate and 1.76 g trisodium citrate in 30 ml dH_2O) and examined by EM (Model CM10, Phillips, Eindoven, Netherlands). Micrographs were captured using a digital camera (model C4742-95, Hamamatsu, Shizuoka, Japan) and Image Capture Engine software (version 5.42.443a, Advanced Microscopy Techniques, Danvers, MA, U.S.A.). The classification of cellular and subcellular elements was based on the descriptions by Peters et al. (1991).

Morris water maze

The Morris water maze was used as described elsewhere (Trinchese et al., 2004; Puzzo et al., 2009). Briefly, mice were trained to learn the location of a hidden platform. A white tank was filled with water (20–22 °C), made opaque with the addition of non-toxic white paint, and a white platform was submerged under the surface of the water. Single-housed mice were trained to locate a hidden platform in 2 daily sessions, 4 h apart for 3 days. Each

session consisted of 3×60 s trials, 30 s apart. The time taken to reach the platform was recorded for each trial and the path was monitored with video tracking to record velocity (HVS 2020; HVS Image, Hampton, UK). On the 4th day, the mice were tested for long-term retention of the platform location using 4 consecutive 60 s probe trials during which the platform was removed. The tank was divided into 4 quadrants and video tracking was used to chart the percent of time the animal spent in the target quadrant containing the platform (quadrant 4). Following the completion of the probe trials, the mice were tested on a visual task to determine if there were differences that could be attributed to vision or swimming velocity. The task consisted of 2 daily sessions for 2 days, 4 h apart. Each session contained 3×60 s trials, 30 s apart. For the visual task, the platform was placed 1 cm above the water, and a small silver feeding bowl was placed in the center of the platform. The platform was moved for each trial. The time to reach the platform was recorded for each trial and video tracking was used to calculate swimming velocity.

Data analysis

For the analysis of weak NeuN-ir, volumes corresponding to regions of weak NeuN-ir are presented as a percentage of the 3-D estimate of total brain volume. For ventricular volume, the outlines of ventricles were traced digitally and used to base a 3-D estimate of total ventricular volume using Bioquant software. For EM, quantification of abnormal mitochondria and myelin defects was performed manually using micrographs. Data are presented as the number of mitochondria per 100 μm^2 of tissue, without correcting for shrinkage, because there was no evidence of differential shrinkage between genotypes (based on observation and calculated ventricular volumes; Table 1). Abnormal mitochondria were defined as previously described (Kong and Xu, 1998; Yazdani et al., 2006; Martin et al., 2007; Boland et al., 2008) using these characteristics: 1) large size, 2) irregular cristae, and 3) irregular or broken outer mitochondrial membranes. Defects in myelination were defined by 1) breaks in the myelin sheath, and 2) redundant whorls of myelin.

Data are presented as mean±standard error of the mean (SEM) and $P<0.05$ was considered significant. Statistical comparisons were made using either a two-tailed Student's *t*-test or two-way analysis of variance (ANOVA; Microsoft Excel 2007, Microsoft Corporation, Redmond, WA, U.S.A.). Prior to ANOVA, Bartlett's test (Snedecor and Cochran, 1989) was used to test for homoscedasticity of variance. Where significant departure from homoscedasticity was detected, this was corrected by log transformation of the data, prior to ANOVA. To analyze the latencies recorded in the hidden trials and probe trial in the water maze, repeated measures analysis of variance (RMANOVA) or ANOVA and Bonferroni/Dunn post-hoc test (Statview v. 5.0.1, SAS Institute Inc., Cary, NC, U.S.A.) were used.

Results

Subjects

$ARMS^{-/-}$ mice that were previously generated by Cre-mediated recombination displayed early embryonic lethality (Wu et al., 2009). Therefore, $ARMS^{+/-}$ mice were used. $ARMS^{+/-}$ mice were viable and fertile and displayed a 30–40% decrease in ARMS protein (Wu et al., 2009).

$ARMS^{+/-}$ mice display abnormal cellular morphology in the EC and FC

Cresyl violet staining was used to screen adult $ARMS^{+/-}$ mice (12-months-old) for detectable defects. There was no evidence of abnormalities except for select cortical regions, notably the EC and FC, and only at high magnification (Figs. 1–3). The cells in the EC of $ARMS^{+/-}$ mice appeared to be pyknotic, i.e., the neurons stained darker than normal, and had a shrunken or deformed appearance (Figs. 1A and B, insets). The pyknotic neurons

appeared to be primarily in the superficial layers (Figs. 1A and B). In adjacent areas of the ARMS$^{+/-}$ mice, and throughout the brain of WT mice, neurons appeared to be relatively normal, i.e., cresyl violet stain was lighter in staining intensity, and the somata did not appear to be shrunken (Fig. 1A). There were no changes in total volume or ventricular volume (Table 1), despite the presence of pyknotic neurons.

Loss of NeuN immunoreactivity is observed in ARMS$^{+/-}$ mice

When areas of pyknotic cells, stained by cresyl violet, were compared to adjacent sections stained with NeuN, the areas where pyknotic cells were evident in one section corresponded to areas with weak NeuN-ir in the adjacent section (Figs. 1B and D; 2). When NeuN labeling was weak, cells were either very lightly labeled by the NeuN antibody, or there was no detectable immunoreactivity, despite the fact that in the same sections there was robust NeuN-ir in adjacent regions (Figs. 1D, 2 and 3C). Therefore, weak NeuN-ir appeared to be a surrogate marker for pyknotic cells.

NeuN-ir was evaluated using computerized thresholding to quantify areas of robust vs. weak NeuN-ir (Figs. 3A and B; for quantification see Fig. 4). Remarkably, there was no evidence of pyknosis or weak NeuN-ir in the hippocampal pyramidal cell layers or the cell layers of the dentate gyrus (Figs. 3A and B). Instead, weak NeuN-ir was found within the adjacent EC, although the location was not always in the exact same subregion of the EC, and sometimes the adjacent areas (e.g., perirhinal cortex) were also affected. In addition, weak NeuN-ir was also present in the FC (FC; see Figs. 3C and D). Remarkably, the EC and FC were the only two areas that were affected across all animals (Figs. 3 and 4). EM was used to confirm that the cells with weak NeuN labeling were in fact present, but abnormal (Figs. 3E and F).

Quantification of weak NeuN-ir showed that the total volume of weak NeuN-ir in the EC was greater in 12-month-old female ARMS$^{+/-}$ mice compared to age-matched female WT mice (WT: 0.31±0.05%, n=6; ARMS$^{+/-}$: 0.69±0.12%, n=5; Student's *t*-test, P=0.0266; Fig. 4B). However, there were no differences in the extent of weak NeuN-ir in the EC of 12-month-old male ARMS$^{+/-}$ mice compared to age-matched male WT mice (WT: 0.49±0.22%, n=4; ARMS$^{+/-}$: 0.56±0.15%, n=4; Student's *t*-test, P=0.833), suggesting that the female EC was affected by ARMS reduction, but not the male EC.

Within the FC, two regions exhibited weak NeuN-ir: 1) an area close to the medial pial membrane (referred to here as the MFC), and 2) an area near the lateral edge of the FC (for the purposes of this study, we refer to this area as the LFC; Figs. 3C and D). Because each part of the MFC and LFC with weak NeuN-ir was always separated by a broad area of robust NeuN-ir, the areas we refer to as MFC and LFC were readily differentiated, and therefore were compared quantitatively. The LFC of female 12-month-old ARMS$^{+/-}$ mice exhibited a significantly greater volume of weak NeuN-ir compared to age-matched female WT mice (WT: 0.07±0.03%, n=6; ARMS$^{+/-}$: 0.32±0.11%, n=5; Student's *t*-test, P=0.0383; Fig. 4B), but the MFC did not (WT: 0.16±0.07%, n=10; ARMS$^{+/-}$: 0.26±0.09%, n=9; Student's *t*-test, P=0.251; Fig. 4B). In male mice at the same age, there were no differences in the volume of weak NeuN-ir, for both the LFC (WT: 0.0.20±0.17%, n=4; ARMS$^{+/-}$: 0.51±0.19%, n=4; Student's *t*-test, P=0.117) and MFC (WT: 0.03±0.02%, n=4; ARMS$^{+/-}$: 0.19±0.16%, n=4; Student's *t*-test, P=0.193), suggesting that the female FC was vulnerable to ARMS reduction but not the male FC.

We also evaluated NeuN-ir at a younger age (1 month) in females (Fig. 4B). ANOVA revealed a significant effect of genotype ($F_{1,13}$ = 8.855, p = 0.011) and of age ($F_{1,13}$ = 8.644 p = 0.012) Therefore, weak NeuN-ir was greater in the ARMS$^{+/-}$ mice than in the WT mice, and the area of weak NeuN-ir was greatest at 12 months of age. However, there was no

age×genotype interaction ($F_{1,13}$ =2.558 p=0.134) so there is no evidence from these data that the increase in weak NeuN-ir with age is genotype-dependent.

Ultrastructural analysis reveals abnormalities in mitochondria and myelination in ARMS$^{+/-}$ mice

Mitochondria—We used EM to investigate the ultrastructural correlates of pyknosis and weak NeuN-ir. In tissue from the EC and FC of ARMS$^{+/-}$ mice, mitochondria appeared to be atypical. Typical mitochondria have a smooth outer membrane enclosing a highly folded inner membrane, forming cristae, and these were observed in the EC and FC of WT mice (Fig. 5A). In the ARMS$^{+/-}$ mice, many mitochondria in the EC and FC had disorganized cristae and irregular outer membranes (Figs. 5B and C). MLBs, consisting of a series of concentrically arranged membranes were also observed (Fig. 5B), were evident in all subcellular compartments, and were not observed in WT mice. Notably, abnormal mitochondria and MLBs have been reported after oxidative stress (Kowaltowski and Vercesi, 1999; Lin and Beal, 2006), retrograde degeneration of nerve cells (Bogolepov, 1971), neurotoxic insults (Yazdani et al., 2006), in a mouse model of amyotrophic lateral sclerosis (Kong and Xu, 1998) and after impaired clearance of autophagosomes (Boland et al., 2008).

To quantify the ultrastructural changes, areas of weak NeuN-ir and strong NeuN-ir in the superficial layers of the lateral EC (LEC) were compared using 12-month-old female WT and ARMS$^{+/-}$ mice (n=5/group; Figs. 4 and 5). The LEC was used for quantification because the LEC was the most common site of weak NeuN-ir within the EC. An area of the LEC that was 2380±499.73 μm^2 was examined per animal. Quantification of the number of abnormal mitochondria (for criteria, see Materials and methods) showed that there were greater numbers in areas of weak NeuN-ir in ARMS$^{+/-}$ mice compared to areas of weak NeuN-ir in WT mice (WT: 0.304±0.220 per 100 μm^2, n=4 mice, ARMS$^{+/-}$: 2.468±0.705 per 100 μm^2, n=5 mice; Student's *t*-test, *P*=0.0402, Fig. 5D). The difference in the number of abnormal mitochondria was also significant when areas of weak NeuN-ir were compared to areas of strong NeuN-ir in ARMS$^{+/-}$ mice (strong NeuN-ir: 0.1364±0.014 per 100 μm^2, n=4 mice, weak NeuN-ir: 2.468±0.705 per 100 μm^2, n=5 mice; Student's *t*-test, *P*=0.0401, Fig. 5D), and areas of strong NeuN-ir in WT mice (WT: 0.105±0.075 per 100 μm^2, n=3 mice, ARMS$^{+/-}$: 2.468±0.705 per 100 μm^2, n=5 mice; Student's *t*-test, *P*=0.0342, Fig. 5D). These results indicate that in ARMS$^{+/-}$ mice, abnormal mitochondria were more frequently detected compared to WT mice, and in areas with weak NeuN-ir, they were more frequent compared to areas with robust NeuN-ir. Thus, areas with abnormal mitochondria corresponded closely to the areas of weak NeuN-ir and pyknotic neurons.

Myelin—In addition to abnormalities of mitochondria, myelin appeared to be defective in ARMS$^{+/-}$ mice (Fig. 6). Specifically, the myelin sheath appeared to contain breaks and redundant whorls of myelin (Figs. 6B and C); these characteristics were used to define abnormal myelin for quantification. Notably, abnormal myelin was located in many areas, in and outside the area of weak NeuN-ir (e.g., regions adjacent to the site of weak NeuN-ir in the EC or FC, including all cortical layers, striatum, hippocampus and the underlying white matter). This was a contrast to the location of abnormal mitochondria, which appeared to be specific for areas of weak NeuN-ir, as explained above. Thus, there were numerous defective myelin profiles in areas of strong and weak NeuN-ir in ARMS$^{+/-}$ mice, and they were not significantly different when quantified per unit area (strong NeuN-ir: 0.807 ± 0.381 per 100 μm^2, n = 4 mice; weak NeuN-ir: 1.854 ±0.627 per 100 μm^2, n = 5 mice; Student's *t*-test, *P* =0.101, Fig. 6D). Taken together, the EM analyses show that the mitochondrial defects exhibited specificity for the areas that had weak NeuN-ir, but abnormal myelin appeared to lack this specificity.

Notably, there were some defects in myelin that were found in 12-month-old WT mice. These occurred in areas with weak or robust NeuN-ir, but were substantially less frequent than in ARMS$^{+/-}$ mice. Thus, the number of these abnormal myelin profiles was less than the number in ARMS$^{+/-}$ mice when areas with weak NeuN-ir were compared (WT: 0.163±0.087 per 100 μm^2, n=3 mice, ARMS$^{+/-}$: 1.854±0.627 per 100 μm^2, n=5 mice; Student's *t*-test, *P*=0.0271, Fig. 6D), or when areas with robust NeuN-ir was compared (WT: 0.137±0.068 per 100 μm^2, n=3 mice, ARMS$^{+/-}$: 1.854±0.627 per 100 μm^2, n=5 mice; Student's *t*-test, *P*=0.0260, Fig. 6D).

Female ARMS$^{+/-}$ mice exhibit deficits in spatial memory

To determine if the anatomical abnormalities in ARMS$^{+/-}$ mice were associated with functional defects, behavioral tests were performed. Female ARMS$^{+/-}$ mice (n=19) were significantly slower to learn the location of the hidden platform during training, compared to female WT mice (n=20). RMANOVA revealed a significant effect of genotype ($F_{1,5}$ =2.835, *P*=0.015) and Bonferroni/Dunn post hoc analysis revealed differences in the 2nd–5th sessions (*P*<0.05; Fig. 7B). However, there was no difference in time to find the hidden platform between 12-month-old male ARMS$^{+/-}$ mice (n=14) and male WT mice (n=14; Fig. 7A).

We also assessed spatial memory with the probe trial (Schenk and Morris, 1985). Female ARMS$^{+/-}$ mice were impaired compared to female WT mice (ANOVA $F_{1,144}$ =5.496, *P* =0.0207; Fig. 7D). However, there was no difference in the amount of time spent in the target quadrant between male ARMS$^{+/-}$ mice and WT mice (Fig. 7C). The visible platform trial, performed after the probe trial, did not reveal any differences in time to reach the platform (males, $F_{1,3}$ =1.143, *P*=0.333; females, $F_{1,3}$ =2.099, *P*=0.101) or swimming velocity (males, $F_{1,3}$ =1.242, *P* =0.295; females, $F_{1,3}$ =0.637, *P* =0.593).

Discussion

Summary

The results demonstrated that ARMS is important to the EC and FC in several ways. First, neurons in the EC and FC were compromised by a decrease in ARMS levels. Second, animals with a reduction in ARMS exhibited deficits in spatial learning and memory, which depend on the EC and FC. Third, the results indicate that females are affected but not males. Taken together, these observations provide support for the hypothesis that neurotrophin signaling is important to the maintenance of normal cortical function, and supports the hypothesis that disruption of neurotrophin signaling contributes to impairments in disorders where areas like the EC and FC are implicated, and women often exhibit a greater incidence or more affective symptoms compared to men (Wizemann and Pardue, 2001).

NeuN-ir is not always a marker of neurons

The results support previous observations that the absence of NeuN-ir does not always indicate neuronal loss. In some circumstances, loss of NeuN immunoreactivity occurs when NeuN is phosphorylated (Igarashi et al., 2001; Davoli et al., 2002; Lind et al., 2005; Portiansky et al., 2006; Buckingham et al., 2008; Matsuda et al., 2009; Won et al., 2009; Wu et al., 2010). The results also show that weak NeuN-ir appears to be a surrogate marker for pyknosis.

Cellular and subcellular abnormalities in the EC and FC of ARMS$^{+/-}$ mice

The cause of pyknosis and weak NeuN-ir in ARMS$^{+/-}$ mice could be related to a type of oxidative stress, given what is known about pyknosis, NeuN-ir, and ARMS. One reason to suggest this is that pyknosis and weak NeuN-ir are often found when there is oxidative stress

(Lemaire et al., 2000; Ünal-Çevik et al., 2004; Portiansky et al., 2006; Buckingham et al., 2008). In addition, our evaluation of ARMS$^{+/-}$ mice showed that cells with weak NeuN-ir had irregular nuclear morphology and mitochondria with abnormal internal membranes. Similar observations have been reported in other studies where oxidative stress occurs (Yakes and Van Houten, 1997; Kong and Xu, 1998; Terni et al., 2010), such as traumatic brain injury (Singh et al., 2006) and neurotoxic insults (Kowaltowski and Vercesi, 1999; Zhu et al., 2007; Rajeswari and Sabesan, 2008). It is interesting that the signs of oxidative stress in ARMS$^{+/-}$ mice were found primarily in the EC and FC, because oxidative damage appears to occur in these areas in neurodegenerative diseases and psychiatric illness. For example, proteins such as mitochondrial adenosine triphosphate-synthase are lipoxidized in the EC during the first stages of AD pathology (Terni et al., 2010). In addition, signs of mitochondrial dysfunction and oxidative stress are also observed in the FC of patients with psychiatric disorders (Michel et al., 2007; Wang et al., 2009; Andreazza et al., 2010; Gawryluk et al., 2010). Therefore, our findings are consistent with a vulnerability of the EC and FC, and the results of this study suggest that a reduction in ARMS plays a role.

The presence of abnormal mitochondria and MLBs is also reminiscent of impaired clearance of damaged organelles by autophagy (Mizushima et al., 2002; Rideout et al., 2004). Autophagy could be impaired in the EC in ARMS$^{+/-}$ mice preferentially because the EC is a metabolically active area, based on studies of cytochrome oxidase (Hevner and Wong-Riley, 1992; Mutisya et al., 1994). A high metabolic rate may lead to a high basal requirement for autophagy, which could place the EC at risk if other insults or injury occur, such as reduced ARMS levels. The importance of autophagy for the maintenance of neuronal integrity has been suggested in the context of other types of insults and injury such as aging and AD (Nixon et al., 2005; Boland and Nixon, 2006; Boland et al., 2008; Finn and Dice, 2008).

Another potential reason for the defects in ARMS$^{+/-}$ mice is related to the myelination defects, because oligodendrocytes are normally dependent on BDNF and TrkB [in spinal cord, (McTigue et al., 1998; Dougherty et al., 2000); in basal forebrain, (Van't Veer et al., 2009) and in retinal ganglion cells, (Cellerino et al., 1997)]. Therefore, the abnormal myelination in ARMS$^{+/-}$ mice may be due to the disruption of BDNF and TrkB signaling. It is possible that myelination is also vulnerable because of the high metabolic activity of oligodendrocytes (McTigue and Tripathi, 2008).

Behavioral impairments in ARMS$^{+/-}$ mice

It was not surprising that there was a defect in the Morris water maze task in female mice, given that this task involves both the EC (Hebert and Dash, 2002; Spowart-Manning and van der Staay, 2005; Nakazawa, 2006) and the FC (Kolb et al., 1983; Jo et al., 2007; Silachev et al., 2009; Leon et al., 2010), and the structural defects were in the EC and FC of female mice. Based on the demonstration that extracellular signal regulated kinase (ERK) in the EC and FC is critical to performance in the Morris water maze (Hebert and Dash, 2002; Leon et al., 2010), and the evidence that ERK is activated by ARMS (Arévalo et al., 2006), reduced ERK activation may also play a role. However, we cannot exclude that other mechanisms that are not ERK-dependent could have contributed, and more experiments will be required to prove that the defects in the EC and FC caused impaired performance. For example, the myelin defects, which were not specific to the EC and FC, but would be likely to affect their functional integration with other brain areas, could have played a role.

Vulnerability of the EC in ARMS$^{+/-}$ mice

The results of this study support the idea that the EC plays a central role in spatial memory normally (Steffenach et al., 2005), that EC pathology develops with aging (Braak and Braak, 1990; Barnes et al., 2000), and that the EC is one of the earliest areas to be affected in AD

(de Leon et al., 2007; de Toledo-Morrell et al., 2007). Interestingly, when the EC was compromised in ARMS$^{+/-}$ mice, the location was primarily the superficial layers. The superficial layers are important because they contain the cells of origin of the EC projection to the hippocampus, the perforant path (Steward and Scoville, 1976; Witter et al., 1989; Dolorfo and Amaral, 1998). In addition, there were myelin defects in ARMS$^{+/-}$ mice which suggests that perforant path axons would be impaired. This is interesting because the defects related to the EC that were observed in clinical studies of patients with AD were related to a deficit in the perforant path axons (de Leon et al., 2007; de Toledo-Morrell et al., 2007), and it was suggested that impairments in the perforant path lead to a "disconnection" of the EC from hippocampus that underlies early cognitive impairment in AD (de Toledo-Morrell et al., 2007).

Sexual dimorphism in ARMS$^{+/-}$ mice

The fact that female mice were affected rather than male mice is interesting because there is evidence for sex differences in spatial memory. Thus, previous studies have documented worse performance by females on spatial memory tasks, not only in rodents (Bucci et al., 1995; La Buda et al., 2002; Gresack and Frick, 2003; Sutcliffe et al., 2007), but also in humans (Perrot-Sinal et al., 1996; Astur et al., 1998, 2004; Postma et al., 1999, 2004), although not all results agree (Bucci et al., 1995). There also are sex differences that have been identified in the perforant path projection, where females appear to exhibit less synaptic plasticity than males (LTP, Maren et al., 1994). Therefore, sex differences that we identified may be due to a specific sexual dimorphism in the normal EC and FC circuits which is revealed in the ARMS$^{+/-}$ mouse. Indeed, the Coolidge effect, where recognition of females by males is critical, is blocked by lesions to the perirhinal cortex/EC, but not lesions to hippocampus (Petrulis and Eichenbaum, 2003). Social odor discrimination in rats appears to depend on EC also (Mayeaux and Johnston, 2004).

Why a reduction in ARMS would increase the vulnerability of EC and FC neurons in females may be related to the normal effects of estrogen in the brain, which increase neurotrophin synthesis (for reviews, see Scharfman and MacLusky, 2005, 2006a). In the EC and FC, estrogen treatment specifically increases neurotrophin levels in females (Bimonte-Nelson et al., 2004). As a result, females may be more dependent on neurotrophins than males, making them more vulnerable to a reduction in ARMS.

Another explanation for the sex difference in ARMS$^{+/-}$ mice is based on the idea that estrogen is not always protective. In transgenic mice that simulate AD pathology, for example, females are more severely affected than males of the same ages (Callahan et al., 2001; Wang et al., 2003; Schuessel et al., 2005; Schafer et al., 2007; Hirata-Fukae et al., 2008). One explanation is based on the idea that estrogen is not protective—and may actually exacerbate damage—when oxidative stress develops (Brinton, 2008; Irwin et al., 2008; Henderson and Brinton, 2010). This is consistent with the findings in the female ARMS$^{+/-}$ mice, where the effect in females was modest before puberty (at 1 month of age) but robust after puberty (at 12 months of age). The normal protective effects of estrogen are also disrupted during aging (Sohrabji and Bake, 2006; Selvamani and Sohrabji, 2008, 2010). An additional contributing factor could be that estrogen increases neuronal activity in the EC (Scharfman and MacLusky, 2005, 2006b; Skucas et al., 2009), which could lead to a greater metabolic demand in the female EC, increasing vulnerability.

Significance

There are many types of neurological and psychiatric disorders that have been related to a deficit in neurotrophins or their receptors (Chao et al., 2006). As a result, it has been suggested that neurotrophic support is necessary to maintain normal CNS function.

However, there are few successful treatment strategies based on neurotrophin signaling at the present time. One reason for the lack of progress in neurotrophin-based therapeutics is that few molecules have been identified that would be specific enough and also have no side effects. For example, BDNF itself can be protective, but has also been associated with seizures (Binder, 2004; Koyama and Ikegaya, 2005; Scharfman, 2005; Tongiorgi et al., 2006; McNamara and Scharfman, 2011). Another reason that therapeutics based on neurotrophins like BDNF have not been implemented is that neurotrophins are large molecules that do not diffuse readily (Thoenen and Sendtner, 2002). Although direct infusion of cells that produce BDNF into areas like the EC has shown great promise (Tuszynski et al., 2005; Nagahara et al., 2009), BDNF itself may not be the best therapeutic molecule. Other neurotrophin based strategies need to be developed. The regulation of ARMS could be one approach to specifically target neurotrophin signaling pathways in areas of the brain that are vulnerable to disease.

Acknowledgments

This study was supported by NIH NS-37562 and MH-084215 to H.E.S., NIH NS-21072 and HD-23315 to M.V.C., NIH AG-034248 to O.A., the New York University Langone Medical Center CoE Seed Grant Program, and the New York State Office of Mental Health. We thank Dr. Ralph Nixon, Dr. Neil Maclusky, Dr. Daniel Wesson, and Patrice Pearce for their suggestions.

References

Andreazza AC, Shao L, Wang JF, Young LT. Mitochondrial complex I activity and oxidative damage to mitochondrial proteins in the prefrontal cortex of patients with bipolar disorder. Arch Gen Psychiatry. 2010; 67:360–368. [PubMed: 20368511]

Arévalo JC, Yano H, Teng KK, Chao MV. A unique pathway for sustained neurotrophin signaling through an ankyrin-rich membrane-spanning protein. EMBO J. 2004; 23:2358–2368. [PubMed: 15167895]

Arévalo JC, Pereira DB, Yano H, Teng KK, Chao MV. Identification of a switch in neurotrophin signaling by selective tyrosine phosphorylation. J Biol Chem. 2006; 281:1001–1007. [PubMed: 16284401]

Arnold SE. Cellular and molecular neuropathology of the parahippocampal region in schizophrenia. Ann N Y Acad Sci. 2000; 911:275–292. [PubMed: 10911880]

Arnold SE, Franz BR, Gur RC, Gur RE, Shapiro RM, Moberg PJ, Trojanowski JQ. Smaller neuron size in schizophrenia in hippocampal subfields that mediate cortical–hippocampal interactions. Am J Psychiatry. 1995; 152:738–748. [PubMed: 7726314]

Astur R, Ortiz M, Sutherland R. A characterization of performance by men and women in a virtual Morris water task: a large and reliable sex difference. Behav Brain Res. 1998; 93:185–190. [PubMed: 9659999]

Astur R, Tropp J, Sava S, Constable R, Markus E. Sex differences and correlations in a virtual Morris water task, a virtual radial arm maze, and mental rotation. Behav Brain Res. 2004; 151:103–115. [PubMed: 15084426]

Barnes CA, Rao G, Houston FP. LTP induction threshold change in old rats at the perforant path–granule cell synapse. Neurobiol Aging. 2000; 21:613–620. [PubMed: 11016529]

Bimonte-Nelson H, Nelson M, Granholm A. Progesterone counteracts estrogen-induced increases in neurotrophins in the aged female rat brain. Neuroreport. 2004; 15:2659–2663. [PubMed: 15570173]

Binder DK. The role of BDNF in epilepsy and other diseases of the mature nervous system. Adv Exp Med Biol. 2004; 548:32–56.

Bogolepov NN. Pathologic inclusions in the mitochondria of neurons undergoing retrograde degeneration (electron microscope study). Zh Nevropatol Psikhiatr Im S S Korsakova. 1971; 71:1337–1341. [PubMed: 4337044]

Boland B, Nixon RA. Neuronal macroautophagy: from development to degeneration. Mol Aspects Med. 2006; 27:503–519. [PubMed: 16999991]

Boland B, Kumar A, Lee S, Platt FM, Wegiel J, Yu WH, Nixon RA. Autophagy induction and autophagosome clearance in neurons: relationship to autophagic pathology in Alzheimer's disease. J Neurosci. 2008; 28:6926–6937. [PubMed: 18596167]

Braak H, Braak E. Neurofibrillary changes confined to the entorhinal region and an abundance of cortical amyloid in cases of presenile and senile dementia. Acta Neuropathol. 1990; 80:479–486. [PubMed: 2251904]

Brinton RD. The healthy cell bias of estrogen action: mitochondrial bioenergetics and neurological implications. Trends Neurosci. 2008; 31:529–537. [PubMed: 18774188]

Bucci D, Chiba AA, Gallagher M. Spatial learning in male and female Long–Evans rats. Behav Neurosci. 1995; 109:180–183. [PubMed: 7734074]

Buckingham BP, Inman DM, Lambert W, Oglesby E, Calkins DJ, Steele MR, Vetter ML, Marsh-Armstrong N, Horner PJ. Progressive ganglion cell degeneration precedes neuronal loss in a mouse model of glaucoma. J Neurosci. 2008; 28:2735–2744. [PubMed: 18337403]

Callahan MJ, Lipinski WJ, Bian F, Durham RA, Pack A, Walker LC. Augmented senile plaque load in aged female beta-amyloid precursor protein-transgenic mice. Am J Pathol. 2001; 158:1173–1177. [PubMed: 11238065]

Cellerino A, Carroll P, Thoenen H, Barde YA. Reduced size of retinal ganglion cell axons and hypomyelination in mice lacking brain-derived neurotrophic factor. Mol Cell Neurosci. 1997; 9:397–408. [PubMed: 9361277]

Chao M, Rajagopal R, Lee F. Neurotrophin signalling in health and disease. Clin Sci (Lond). 2006; 110:167–173. [PubMed: 16411893]

Davoli MA, Fourtounis J, Tam J, Xanthoudakis S, Nicholson D, Robertson GS, Ng GYK, Xu D. Immunohistochemical and biochemical assessment of caspase-3 activation and DNA fragmentation following transient focal ischemia in the rat. Neuroscience. 2002; 115:125–136. [PubMed: 12401327]

de Leon MJ, Mosconi L, Blennow K, de Santi S, Zinkowski R, Mehta PD, Pratico D, Tsui W, Saint Louis LA, Sobanska L, Brys M, Li Y, Rich K, Rinne J, Rusinek H. Imaging and CSF studies in the preclinical diagnosis of Alzheimer's disease. Ann N Y Acad Sci. 2007; 1097:114–145. [PubMed: 17413016]

de Toledo-Morrell L, Goncharova I, Dickerson B, Wilson RS, Bennett DA. From healthy aging to early Alzheimer's disease: *in vivo* detection of entorhinal cortex atrophy. Ann N Y Acad Sci. 2000; 911:240–253. [PubMed: 10911878]

de Toledo-Morrell L, Stoub TR, Wang C. Hippocampal atrophy and disconnection in incipient and mild Alzheimer's disease. Prog Brain Res. 2007; 163:741–753. [PubMed: 17765748]

Dolorfo CL, Amaral DG. Entorhinal cortex of the rat: organization of intrinsic connections. J Comp Neurol. 1998; 398:49–82. [PubMed: 9703027]

Dougherty KD, Dreyfus CF, Black IB. Brain-derived neurotrophic factor in astrocytes, oligodendrocytes, and microglia/macrophages after spinal cord injury. Neurobiol Dis. 2000; 7:574–585. [PubMed: 11114257]

Drevets WC. Functional anatomical abnormalities in limbic and prefrontal cortical structures in major depression. Prog Brain Res. 2000; 126:413–431. [PubMed: 11105660]

Du F, Whetsell WOJ, Abou-Khalil B, Blumenkopf B, Lothman E, Schwarcz R. Preferential neuronal loss in layer III of the entorhinal cortex in patients with temporal lobe epilepsy. Epilepsy Res. 1993; 16:223–233. [PubMed: 8119273]

Duffy AM, Zhou P, Milner TA, Pickel VM. Spatial and intracellular relationships between the alpha7 nicotinic acetylcholine receptor and the vesicular acetylcholine transporter in the prefrontal cortex of rat and mouse. Neuroscience. 2009; 161:1091–1103. [PubMed: 19374941]

Durany N, Michel T, Zöchling R, Boissl KW, Cruz-Sánchez FF, Riederer P, Thome J. Brain-derived neurotrophic factor and neurotrophin 3 in schizophrenic psychoses. Schizophr Res. 2001; 52:79–86. [PubMed: 11595394]

Finn PF, Dice JF. Proteolytic and lipolytic responses to starvation. Nutrition. 2008; 22:830–844. [PubMed: 16815497]

Gawryluk JW, Wang JF, Andreazza AC, Shao L, Young LT. Decreased levels of glutathione, the major brain antioxidant, in post-mortem prefrontal cortex from patients with psychiatric disorders. Int J Neuropsychopharmacol. 2010; 16:1–8.

Gomez-Isla T, Price JL, McKeel DW Jr, Morris JC, Growdon JH, Hyman BT. Profound loss of layer II entorhinal cortex neurons occurs in very mild Alzheimer's disease. J Neurosci. 1996; 16:4491–4500. [PubMed: 8699259]

Gresack J, Frick KM. Male mice exhibit better spatial working and reference memory than females in a water-escape radial arm maze task. Brain Res. 2003; 982:98–107. [PubMed: 12915244]

Hayakawa N, Yokoyama H, Kato H, Araki T. Age-related alterations of oxidative stress markers in the mouse hippocampal CA1 sector. Exp Mol Pathol. 2008; 85:135–140. [PubMed: 18586238]

Hebert AE, Dash PK. Extracellular signal-regulated kinase activity in the entorhinal cortex is necessary for long-term spatial memory. Learn Mem. 2002; 9:156–166. [PubMed: 12177229]

Henderson V, Brinton R. Menopause and mitochondria: windows into estrogen effects on Alzheimer's disease risk and therapy. Prog Brain Res. 2010; 182:77–96. [PubMed: 20541661]

Hevner RF, Wong-Riley MT. Entorhinal cortex of the human, monkey, and rat: metabolic map as revealed by cytochrome oxidase. J Comp Neurol. 1992; 326:451–469. [PubMed: 1334980]

Hirata-Fukae C, Li HF, Hoe HS, Gray AJ, Minami SS, Hamada K, Niikura T, Hua F, Tsukagoshi-Nagai H, Horikoshi-Sakuraba Y, Mughal M, Rebeck GW, LaFerla FM, Mattson MP, Iwata N, Saido TC, Klein WL, Duff KE, Aisen PS, Matsuoka Y. Females exhibit more extensive amyloid, but not tau, pathology in an Alzheimer transgenic model. Brain Res. 2008; 1216:92–103. [PubMed: 18486110]

Holland D, Brewer JB, Hagler DJ, Fenema-Notestine C, Dale AM. Subregional neuroanatomical change as a biomarker for Alzheimer's disease. Proc Natl Acad Sci U S A. 2009; 106:20954–20959. [PubMed: 19996185]

Igarashi T, Huang TT, Noble LJ. Regional vulnerability after traumatic brain injury: gender differences in mice that overexpress human copper, zinc superoxide dismutase. Exp Neurol. 2001; 172:332–341. [PubMed: 11716557]

Iglesias T, Cabrera-Poch N, Mitchell MP, Naven TJP, Rozengurt E, Schiavo G. Identification and cloning of kidins220, a novel neuronal substrate of protein kinase D. J Biol Chem. 2000; 275:40048–40056. [PubMed: 10998417]

Irwin R, Yao J, Hamilton R, Cadenas E, Brinton R, Nilsen J. Progesterone and estrogen regulate oxidative metabolism in brain mitochondria. Endocrinology. 2008; 149:167–175.

Jo YS, Park EH, Kim IH, Park SK, Kim H, Kim HT, Choi JS. The medial prefrontal cortex is involved in spatial memory retrieval under partial-cue conditions. J Neurosci. 2007; 27:13567–13578. [PubMed: 18057214]

Kadriu B, Guidotti A, Costa E, Auta J. Imidazenil, a non-sedating anticonvulsant benzodiazepine, is more potent than diazepam in protecting against DFP-induced seizures and neuronal damage. Toxicology. 2009; 256:164–174. [PubMed: 19111886]

Knusel B, Gao H. Neurotrophins and Alzheimer's disease: beyond the cholinergic neurons. Life Sci. 1996; 58:2019–2027. [PubMed: 8637432]

Kolb B, Sutherland R, Whishaw I. A comparison of the contributions of the frontal and parietal association cortex to spatial localization in rats. Behav Neurosci. 1983; 97:13–37. [PubMed: 6838719]

Kong J, Xu Z. Massive mitochondrial degeneration in motor neurons triggers the onset of amyotrophic lateral sclerosis in mice expressing a mutant SOD1. J Neurosci. 1998; 18:3241–3250. [PubMed: 9547233]

Kong H, Boulter J, Weber JL, Lai C, Chao MV. An evolutionarily conserved transmembrane protein that is a novel downstream target of neurotrophin and ephrin receptors. J Neurosci. 2001; 21:176–185. [PubMed: 11150334]

Kordower J, Chu Y, Stebbins G, DeKosky S, Cochran E, Bennett D, Mufson E. Loss and atrophy of layer II entorhinal cortex neurons in elderly people with mild cognitive impairment. Ann Neurol. 2001; 49:202–213. [PubMed: 11220740]

Kowaltowski AJ, Vercesi AE. Mitochondrial damage induced by conditions of oxidative stress. Free Radic Biol Med. 1999; 26:463–471. [PubMed: 9895239]

Koyama R, Ikegaya Y. To BDNF or not to BDNF: that is the epileptic hippocampus. Neuroscientist. 2005; 11:282–287. [PubMed: 16061515]

Krimer LS, Herman MM, Saunders RC, Boyd JC, Hyde TM, Carter JM, Kleinman JE, Weinberger DR. A qualitative and quantitative analysis of the entorhinal cortex in schizophrenia. Cereb Cortex. 1997; 7:732–739. [PubMed: 9408037]

La Buda C, Mellgren R, Hale R. Sex differences in the acquisition of a radial maze task in the CD-1 mouse. Physiol Behav. 2002; 76:213–217. [PubMed: 12044593]

Lai KO, Ip NY. Synapse development and plasticity: roles of ephrin/Eph receptor signaling. Curr Opin Neurobiol. 2009; 19:275–283. [PubMed: 19497733]

Lemaire V, Koehl M, Le Moal M, Abrous DN. Prenatal stress produces learning deficits associated with an inhibition of neurogenesis in the hippocampus. Proc Natl Acad Sci U S A. 2000; 97:11032–11037. [PubMed: 11005874]

Leon WC, Bruno MA, Allard S, Nader K, Cuello AC. Engagement of the PFC in consolidation and recall of recent spatial memory. Cereb Cortex. 2010; 17:297–305.

Lewis DA, Glantz LA, Pierri JN, Sweet RA. Altered cortical glutamate neurotransmission in schizophrenia. Ann N Y Acad Sci. 2003; 1003:102–112. [PubMed: 14684438]

Lin MT, Beal MF. Mitochondrial dysfunction and oxidative stress in neurodegenerative diseases. Nature. 2006; 443:787–795. [PubMed: 17051205]

Lind D, Franken S, Kappler J, Jankowski J, Schilling K. Characterization of the neuronal marker NeuN as a multiply phosphorylated antigen with discrete subcellular localization. J Neurosci Res. 2005; 79:295–302. [PubMed: 15605376]

Lindvall O, Kokaia Z, Bengzon J, Elmér E, Kokaia M. Neurotrophins and brain insults. Trends Neurosci. 1994; 17:490–496. [PubMed: 7531892]

Lopez-Menendez C, Gascon S, Sobrado M, Vidaurre OG, Higuero AM, Rodriguez-Pena A, Iglesias T, Diaz-Guerra M. Kidins220/ARMS downregulation by excitotoxic activation of NMDARs reveals its involvement in neuronal survival and death pathways. J Cell Sci. 2009; 122:3554–3565. [PubMed: 19759287]

Maren S, De Oca B, Fanselow M. Sex differences in hippocampal long-term potentiation (LTP) and Pavlovian fear conditioning in rats: positive correlation between LTP and contextual learning. Brain Res. 1994; 661:25–34. [PubMed: 7834376]

Martin LJ, Liu Z, Chen K, Price AC, Pan Y, Swaby JA, Golden WC. Motor neuron degeneration in amyotrophic lateral sclerosis mutant superoxide dis-mutase-1 transgenic mice: mechanisms of mitochondriopathy and cell death. J Comp Neurol. 2007; 500:20–46. [PubMed: 17099894]

Matsuda S, Umeda M, Uchida H, Kato H, Araki T. Alterations of oxidative stress markers and apoptosis markers in the striatum after transient focal cerebral ischemia in rats. J Neural Transm. 2009; 116:395–404. [PubMed: 19238518]

Mayeaux D, Johnston R. Discrimination of social odors and their locations: role of lateral entorhinal area. Physiol Behav. 2004; 82:653–662. [PubMed: 15327913]

McDonald CR, McEvoy LK, Gharapetian L, Fennema-Notestine C, Hagler DJ Jr, Holland D, Koyama A, Brewer JB, Dale AM. Regional rates of neocortical atrophy from normal aging to early Alzheimer disease. Neurology. 2009; 73:457–465. [PubMed: 19667321]

McNamara, JO.; Scharfman, HE., editors. Temporal Lobe Epilepsy and the BDNF Receptor, TrkB. Oxford; Oxford: 2011.

McTigue DM, Tripathi RB. The life, death, and replacement of oligodendrocytes in the adult CNS. J Neurochem. 2008; 107:1–19. [PubMed: 18643793]

McTigue DM, Horner PJ, Stokes BT, Gage FH. Neurotrophin-3 and brain-derived neurotrophic factor induce oligodendrocyte proliferation and myelination of regenerating axons in the contused adult rat spinal cord. J Neurosci. 1998; 18:5354–5365. [PubMed: 9651218]

Michel TM, Frangou S, Thiemeyer D, Camara S, Jecel J, Nara K, Brunklaus A, Zoechling R, Riederer P. Evidence for oxidative stress in the frontal cortex in patients with recurrent depressive disorder — a postmortem study. Psychiatry Res. 2007; 151:145–150. [PubMed: 17296234]

Mizushima N, Ohsumi Y, Yoshimori T. Autophagosome formation in mammalian cells. Cell Struct Funct. 2002; 27:421–429. [PubMed: 12576635]

Mullen RJ, Buck CR, Smith AM. NeuN, a neuronal specific nuclear protein in vertebrates. Development. 1992; 116:201–211. [PubMed: 1483388]

Murai KK, Pasquale EB. Eph receptors, ephrins, and synaptic function. Neuroscientist. 2004; 10:304–314. [PubMed: 15271258]

Mutisya EM, Bowling AC, Beal MF. Cortical cytochrome oxidase activity is reduced in Alzheimer's disease. J Neurochem. 1994; 63:2179–2184. [PubMed: 7964738]

Nagahara AH, Merrill DA, Coppola G, Tsukada S, Schroeder BE, Shaked GM, Wang L, Blesch A, Kim A, Conner JM, Rockenstein E, Chao MV, Koo EH, Geschwind D, Masliah E, Chiba AA, Tuszynski MH. Neuroprotective effects of brain-derived neurotrophic factor in rodent and primate models of Alzheimer's disease. Nat Med. 2009; 15:331–337. [PubMed: 19198615]

Nakazawa K. Inducible and cell-type restricted manipulation in the entorhinal cortex. Neuron. 2006; 50:183–185. [PubMed: 16630829]

Nixon RA, Wegiel J, Kumar A, Yu WH, Peterhoff C, Cataldo A, Cuervo AM. Extensive involvement of autophagy in Alzheimer disease: an immuno-electron microscopy study. J Neuropathol Exp Neurol. 2005; 62:113–122. [PubMed: 15751225]

Paxinos, G.; Franklin, KBJ. The Mouse Brain in Stereotaxic Coordinates. Academic Press; San Diego: 2001.

Peng S, Garzon DJ, Marchese M, Klein W, Ginsberg SD, Francis BM, Mount HTJ, Mufson EJ, Salehi A, Fahnestock M. Decreased brain-derived neurotrophic factor depends on amyloid aggregation state in transgenic mouse models of Alzheimer's disease. J Neurosci. 2009; 29:9321–9329. [PubMed: 19625522]

Perrot-Sinal T, Kostenuik M, Ossenkopp K, Kavaliers M. Sex differences in performance in the Morris water maze and the effects of initial nonstationary hidden platform training. Behav Neurosci. 1996; 110:1309–1320. [PubMed: 8986334]

Peters, A.; Palay, SL.; Webster, HD. The Fine Structure of the Nervous System. Oxford University Press; New York: 1991.

Petrulis A, Eichenbaum H. The perirhinal–entorhinal cortex, but not the hippocampus, is critical for expression of individual recognition in the context of the Coolidge effect. Neuroscience. 2003; 122:599–607. [PubMed: 14622903]

Portiansky EL, Barbeito CG, Gimeno EJ, Zuccolilli GO, Goya RG. Loss of NeuN immunoreactivity in rat spinal cord neurons during aging. Exp Neurol. 2006; 202:519–521. [PubMed: 16935281]

Postma A, Winkel J, Tuiten A, van Honk J. Sex differences and menstrual cycle effects in human spatial memory. Psychoneuroendocrinology. 1999; 24:175–192. [PubMed: 10101726]

Postma A, Jager G, Kessels R, Koppeschaar H, van Honk J. Sex differences for selective forms of spatial memory. Brain Cogn. 2004:54. [PubMed: 15134843]

Puzzo D, Staniszewski A, Deng SX, Privitera L, Leznik E, Liu S, Zhang H, Feng Y, Palmeri A, Landry DW, Arancio O. Phosphodiesterase 5 inhibition improves synaptic function, memory, and amyloid-β load in an Alzheimer's disease mouse model. J Neurosci. 2009; 29:8075–8086. [PubMed: 19553447]

Rajeswari A, Sabesan M. Neuropathological changes induced by neurotoxin 1-methyl-4-phenyl-1,2,3,6-tetrahydropyridine in male Swiss albino mice. Toxicol Ind Health. 2008; 24:189–194. [PubMed: 18842698]

Rajkowska G. Cell pathology in bipolar disorder. Bipolar Disord. 2002; 4:105–116. [PubMed: 12071508]

Rideout HJ, Lang-Rollin I, Stefanis L. Involvement of macroautophagy in the dissolution of neuronal inclusions. Int J Biochem Cell Biol. 2004; 36:2551–2562. [PubMed: 15325592]

Schafer S, Wirths O, Multhaup G, Bayer TA. Gender dependent APP processing in a transgenic mouse model of Alzheimer's disease. J Neural Transm. 2007; 114:387–394. [PubMed: 17075721]

Scharfman HE. Epileptogenesis in the parahippocampal region: parallels with the dentate gyrus. Ann N Y Acad Sci. 2000; 911:305–327. [PubMed: 10911882]

Scharfman HE. Brain-derived neurotrophic factor and epilepsy — a missing link? Epilepsy Curr. 2005; 5:83–88. [PubMed: 16145610]

Scharfman HE, MacLusky NJ. Similarities between actions of estrogen and BDNF in the hippocampus: coincidence or clue? Trends Neurosci. 2005; 28:79–85. [PubMed: 15667930]

Scharfman HE, MacLusky NJ. Estrogen and brain-derived neurotrophic factor (BDNF) in hippocampus: complexity of steroid hormone-growth factor interactions in the adult CNS. Front Neuroendocrinol. 2006a; 27:415–435. [PubMed: 17055560]

Scharfman HE, MacLusky NJ. The influence of gonadal hormones on neuronal excitability, seizures, and epilepsy in the female. Epilepsia. 2006b; 47:1423–1440. [PubMed: 16981857]

Scharfman HE, Sollas AL, Smith KL, Jackson MB, Goodman JH. Structural and functional asymmetry in the normal and epileptic rat dentate gyrus. J Comp Neurol. 2002; 454:424–439. [PubMed: 12455007]

Scharfman HE, Mercurio TC, Goodman JH, Wilson MA, MacLusky NJ. Hippocampal excitability increases during the estrous cycle in the rat: a potential role for brain-derived neurotrophic factor. J Neurosci. 2003; 23:11641–11652. [PubMed: 14684866]

Scharfman HE, Malthankar-Phatak GH, Friedman D, Pearce P, McCloskey DP, Harden CL, MacLusky NJ. A rat model of epilepsy in women: a tool to study physiological interactions between endocrine systems and seizures. Endocrinology. 2009; 150:4437–4442. [PubMed: 19443573]

Schenk F, Morris RGM. Dissociation between components of spatial memory in rats after recovery from the effects of retrohippocampal lesions. Exp Brain Res. 1985; 58:11–28. [PubMed: 3987843]

Schroeter ML, Stein T, Maslowski N, Neumann J. Neural correlates of Alzheimer's disease and mild cognitive impairment: a systematic and quantitative meta-analysis involving 1351 patients. Neuroimage. 2009; 47:1196–1206. [PubMed: 19463961]

Schuessel K, Schafer S, Bayer TA, Czech C, Pradier L, Muller-Spahn F, Muller WE, Eckert A. Impaired Cu/Zn-SOD activity contributes to increased oxidative damage in APP transgenic mice. Neurobiol Dis. 2005; 18:89–99. [PubMed: 15649699]

Selvamani A, Sohrabji F. Reproductive age modulates the impact of focal ischemia on the forebrain as well as the effects of estrogen treatment in female rats. Neurobiol Aging. 2008; 31:1618–1628. [PubMed: 18829137]

Selvamani A, Sohrabji F. The neurotoxic effects of estrogen on ischemic stroke in older female rats is associated with age-dependent loss of insulin-like growth factor-1. J Neurosci. 2010; 30:6852–6861. [PubMed: 20484627]

Shah PJ, Glabus MF, Goodwin GM, Ebmeier KP. Chronic, treatment-resistant depression and right fronto-striatal atrophy. Br J Psychiatry. 2002; 180:434–440. [PubMed: 11983641]

Shoval G, Weizman A. The possible role of neurotrophins in the pathogenesis and therapy of schizophrenia. Eur Neuropsychopharmacol. 2005; 15:319–329. [PubMed: 15820422]

Silachev D, Shram S, Shakova F, Romanova G, Myasoedov N. Formation of spatial memory in rats with ischemic lesions to the prefrontal cortex; effects of a synthetic analog of ACTH(4–7). Neurosci Behav Physiol. 2009; 39:749–756. [PubMed: 19779827]

Singh IN, Sullivan PG, Deng Y, Mbye LH, Hall ED. Time course of post-traumatic mitochondrial oxidative damage and dysfunction in a mouse model of focal traumatic brain injury: implications for neuroprotective therapy. J Cereb Blood Flow Metab. 2006; 26:1407–1418. [PubMed: 16538231]

Skucas, V.; MacLusky, NJ.; Scharfman, HE. 2009 Neuroscience Meeting Planner. Society for Neuroscience; Chicago, IL: 2009. Potent effects of reproductive steroids in the rat entorhinal cortex Program No. 773.4. Online

Snedecor, GW.; Cochran, WG. Statistical Methods. Iowa State University Press; Ames: 1989.

Sniderhan LF, Stout A, Lu Y, Chao MV, Maggirwar SB. Ankyrin-rich membrane spanning protein plays a critical role in nuclear factor-κb signaling. Mol Cell Neurosci. 2008; 38:404–416. [PubMed: 18501627]

Sohrabji F, Bake S. Age-related changes in neuroprotection: is estrogen pro-inflammatory for the reproductive senescent brain? Endocr. 2006; 29:191–197.

Spowart-Manning L, van der Staay FJ. Spatial discrimination deficits by excitotoxic lesions in the Morris water escape task. Behav Brain Res. 2005; 156:269–276. [PubMed: 15582113]

Steffenach HA, Witter M, Moser MB, Moser EI. Spatial memory in the rat requires the dorsolateral band of the entorhinal cortex. Neuron. 2005; 45:301–313. [PubMed: 15664181]

Steward O, Scoville SA. Cells of origin of entorhinal cortical afferents to the hippocampus and fascia dentata of the rat. J Comp Neurol. 1976; 169:347–370. [PubMed: 972204]

Sutcliffe J, Marshall KM, Neill JC. Influence of gender on working and spatial memory in the novel object recognition task in the rat. Behav Brain Res. 2007; 177:117–125. [PubMed: 17123641]

Tapia-Arancibia L, Aliaga E, Silhol M, Arancibia S. New insights into brain BDNF function in normal aging and Alzheimer disease. Brain Res Rev. 2008; 59:201–220. [PubMed: 18708092]

Terni B, Boada J, Portero-Otin M, Pamplona R, Ferrer I. Mitochondrial ATP-synthase in the entorhinal cortex is a target of oxidative stress at stages I/II of Alzheimer's disease pathology. Brain Pathol. 2010; 20:222–233. [PubMed: 19298596]

Thoenen H, Sendtner M. Neurotrophins: from enthusiastic expectations through sobering experiences to rational therapeutic approaches. Nat Neurosci. 2002; 5:1046–1050. [PubMed: 12403983]

Tongiorgi E, Domenici L, Simonato M. What is the biological significance of BDNF mRNA targeting in the dendrites? Mol Neurobiol. 2006; 33:17–32. [PubMed: 16388108]

Trinchese F, Liu S, Battaglia F, Walter S, Mathews PM, Arancio O. Progressive age-related development of Alzheimer-like pathology in APP/PS1 mice. Ann Neurol. 2004; 55:801–814. [PubMed: 15174014]

Tuszynski MH, Thal L, Pay M, Salmon DP, UHS, Bakay R, Patel P, Blesch A, Vahlsing HL, Ho G, Tong G, Potkin SG, Fallon J, Hansen L, Mufson EJ, Kordower JH, Gall C, Conner J. A phase 1 clinical trial of nerve growth factor gene therapy for Alzheimer disease. Nat Med. 2005; 11:551–555. [PubMed: 15852017]

Ünal-Çevik I, KilInç M, Gürsoy-Özdemir Y, Gurer G, Dalkara T. Loss of NeuN immunoreactivity after cerebral ischemia does not indicate neuronal cell loss: a cautionary note. Brain Res. 2004; 1015:169–174. [PubMed: 15223381]

Van't Veer A, Du Y, Fischer TZ, Boetig DR, Wood MR, Dreyfus CF. Brain-derived neurotrophic factor effects on oligodendrocyte progenitors of the basal forebrain are mediated through TrkB and the MAP kinase pathway. J Neurosci Res. 2009; 87:69–78. [PubMed: 18752299]

Wang J, Tanila H, Puolivali J, Kadish I, van Groen T. Gender differences in the amount and deposition of amyloidbeta in APPswe and PS1 double transgenic mice. Neurobiol Dis. 2003; 14:318–327. [PubMed: 14678749]

Wang JF, Shao L, Sun X, Young LT. Increased oxidative stress in the anterior cingulate cortex of subjects with bipolar disorder and schizophrenia. Bipolar Disord. 2009; 11:523–529. [PubMed: 19624391]

Weickert CS, Hyde TM, Lipska BK, Herman MM, Weinberger DR, Kleinman JE. Reduced brain-derived neurotrophic factor in prefrontal cortex of patients with schizophrenia. Mol Psychiatry. 2003; 8:592–610. [PubMed: 12851636]

Weickert CS, Ligons DL, Romancyzk T. Reductions in neurotrophin receptor mRNAs in the prefrontal cortex of patients with schizophrenia. Mol Psychiatry. 2005; 10:637–650. [PubMed: 15940304]

Whitten WK, Bronson FH, Greenstein JA. Estrus-inducing pheromone of male mice: transport by movement of air. Science. 1968; 161:584–585. [PubMed: 5690897]

Winawer MR, Makarenko N, McCloskey DP, Hintz TM, Nair N, Palmer AA, Scharfman HE. Acute and chronic responses to the convulsant pilocarpine in DBA/2 J and A/J mice. Neuroscience. 2007; 149:465–475. [PubMed: 17904758]

Witter MP, Groenewegen HJ, Lopes da Silva FH, Lohman AHM. Functional organization of the extrinsic and intrinsic circuitry of the parahippocampal region. Prog Neurobiol. 1989; 33:161–253. [PubMed: 2682783]

Wizemann, T.; Pardue, M. Committee on Understanding the Biology of Sex and Gender Differences. National Academy Press; Washington, D.C: 2001. Exploring the biological contributions to human health: does sex matter?.

Won SY, Choi SH, Jin BK. Prothrombin kringle-2-induced oxidative stress contributes to the death of cortical neurons in vivo and in vitro: role of microglial NADPH oxidase. J Neuroimmunol. 2009; 214:83–92. [PubMed: 19660816]

Wu SH, Arévalo JC, Sarti F, Tessarollo L, Gan WB, Chao MV. Ankyrin repeat-rich membrane spanning/kidins220 protein regulates dendritic branching and spine stability *in vivo*. Dev Neurobiol. 2009; 69:547–557. [PubMed: 19449316]

Wu KL, Li YQ, Tabassum A, Lu WY, Aubert I, Wong CS. Loss of neuronal protein expression in mouse hippocampus after irradiation. J Neuropathol Exp Neurol. 2010; 69:272–280. [PubMed: 20142763]

Yakes FM, Van Houten B. Mitochondrial DNA damage is more extensive and persists longer than nuclear DNA damage in human cells following oxidative stress. Proc Natl Acad Sci U S A. 1997; 94:514–519. [PubMed: 9012815]

Yazdani U, German DC, Liang CL, Manzino L, Sonsalla PK, Zeevalk GD. Rat model of Parkinson's disease: chronic central delivery of 1-methyl-4-phenylpyr-idinium (MPP+). Exper Neurol. 2006; 200:172–183. [PubMed: 16546169]

Zhu JH, Horbinski C, Guo F, Watkins S, Uchiyama Y, Chu CT. Regulation of autophagy by extracellular signal-regulated protein kinases during 1-methyl-4-phenylpyridinium-induced cell death. Am J Pathol. 2007; 170:75–86. [PubMed: 17200184]

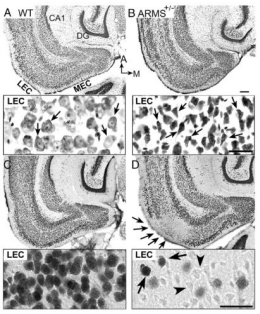

Fig. 1.

Pyknotic neurons and weak NeuN-immunoreactivity in the entorhinal cortex (EC) of ARMS$^{+/-}$ mice. (A) A horizontal section showing the lateral EC (LEC) from a WT mouse, stained with cresyl violet. MEC = medial EC; CA1 = area CA1; DG = dentate gyrus; A = anterior; M = medial. Inset: Layer II/III of the LEC shown at higher power. Arrows point to cresyl violet stained neurons with normal morphology. (B) A cresyl violet-stained section from an ARMS$^{+/-}$ mouse, from a similar dorso-ventral level to (A). Inset: Arrows point to layer II/III neurons from the LEC that appear to be pyknotic because they are darkly stained, and somata are shrunken, with angular edges. (C) A section labeled using an antibody to NeuN that was adjacent to the one in A shows normal NeuN-immunoreactivity (ir). Inset: Layer II/III of the LEC illustrates normal NeuN-ir labeling. (D) A NeuN-labeled section that was adjacent to the section in B shows weak NeuN-ir, primarily in the superficial layers of the LEC (arrows). Inset: Layer II/III of the LEC is shown at higher power. Many cells show weak or no NeuN-ir (arrowheads) in contrast to some cells with normal NeuN-ir (arrows). Calibration for A–D (shown in B)=100 μm; calibration for insets in A–B (shown in inset for B)=25 μm, and calibration for insets in C–D (shown in inset for D)=25 μm.

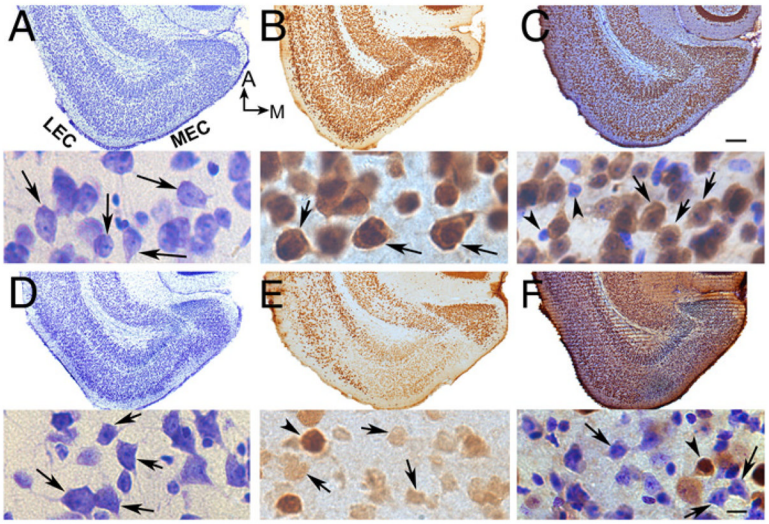

Fig. 2.

Weak NeuN immunoreactivity as a surrogate marker of pyknotic cells. (A) A horizontal section showing the EC and surrounding areas from a WT mouse, stained with cresyl violet. MEC=medial EC; A=anterior; M=medial. Inset: Layers II/III of the LEC shown at higher power. Arrows point to cresyl violet-stained neurons in layers II/III with normal morphology. Calibration for A–F (shown in C)=200 μm; calibration for insets in A–F (shown in inset for F)=20 μm. (B) NeuN-ir in a section adjacent to the one in part A shows normal NeuN-ir. Inset: Cells in layer II/III of the LEC exhibit robust NeuN-ir (arrows). (C) A section adjacent to the one in part B labeled with NeuN and counterstained with cresyl violet. Inset: Cells in layer II/III of the LEC are labeled with NeuN and stained with cresyl violet (arrows). Cells that are stained with cresyl violet only and have small irregular profiles are presumably glia (arrowheads). (D) A cresyl violet-stained section from an $ARMS^{+/-}$ mouse at a similar dorso-ventral level as the WT mouse (A–C). Inset: Arrows point to cells in layers II/III of the LEC that appear to be pyknotic because their somata are shrunken and have angular edges. (E) A NeuN-labeled section that was 150 μm ventral to the section in D shows weak NeuN-ir the EC. Inset: Cells in layers II/III in the LEC are shown at higher power. Many cells with weak or no detectable NeuN-ir (arrows) are present, but some cells exhibit strong NeuN-ir (arrowhead). (F) A section adjacent to the one in D labeled with NeuN and counterstained with cresyl violet. Inset: Arrows point to layer II/III cells of the LEC that appear pyknotic and lack NeuN-ir. Some cells are labeled by cresyl violet and have robust NeuN-ir (arrowhead). (For interpretation of the references to color in this figure legend, the reader is referred to the web version of this article.)

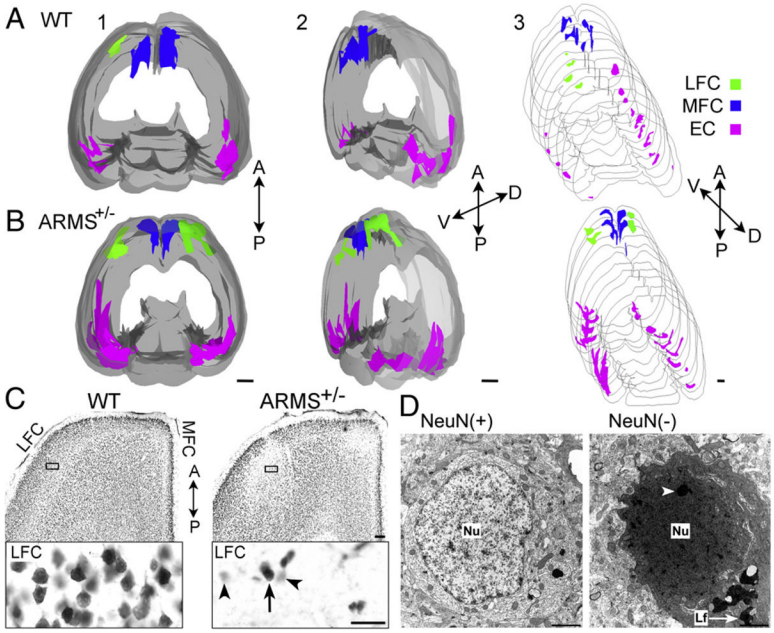

Fig. 3.

Quantification of NeuN-ir in WT and ARMS$^{+/-}$ mice. (A and B) Representative examples of WT (A) and ARMS$^{+/-}$ (B) mice are shown. All sections from the animals that were used for Figs. 1 and 2 were merged to create 3-D images of the entire brain and are shown with different orientations (1–3) as indicated by the axes to the right of each reconstruction. Areas of weak NeuN-ir, detected by computerized thresholding, are shown in color (green = LFC; blue = MFC; pink = EC and adjacent areas). Areas of robust NeuN-ir are shown in gray. A = anterior; P = posterior, V = ventral, D = dorsal. Calibrations in 1–3=1 mm. (C) A NeuN-labeled horizontal section shows normal NeuN-ir of the FC of a WT mouse (left) and weak NeuN-ir in the FC of an ARMS$^{+/-}$ mouse (right). LFC = lateral FC; MFC = medial FC. Inset: The area that is outlined by a box is shown at higher power. A cell with strong NeuN-ir is marked by an arrow; cells with weak NeuN-ir are marked by arrowheads. Calibration for C=100 μm; calibration for insets in C=25 μm. (D) An electron micrograph of a cell with strong NeuN-ir (left; NeuN-positive or NeuN (+)) exhibits normal ultrastructure, whereas a cell with weak NeuN-ir (right; NeuN-negative or NeuN (−)) exhibits abnormal characteristics. The nucleus (Nu) is shrunken and there is clumping of nuclear chromatin (white arrowhead). Lf = lipofuscin bodies. Calibration=500 nm. (For interpretation of the references to color in this figure legend, the reader is referred to the web version of this article.)

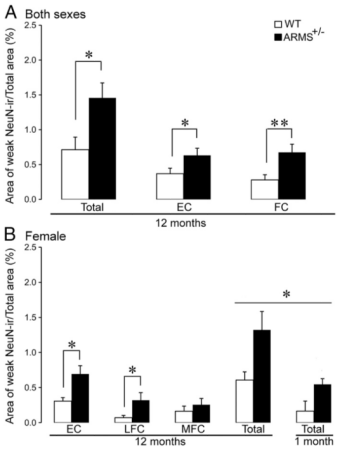

Fig. 4.

Quantification of weak NeuN-ir in ARMS$^{+/-}$ mice compared to WT mice. (A) The total volumes of weak NeuN-ir in the EC and FC are shown for 12-month-old ARMS$^{+/-}$ mice (black) and WT controls (white). Single asterisk indicates $P<0.05$; double asterisk indicates $P<0.01$(for statistics, see text). (B) Comparisons are shown for the EC, LFC and MFC of female ARMS$^{+/-}$ mice and female WT controls. There is a greater volume of weak NeuN-ir in the EC and LFC of ARMS$^{+/-}$ mice compared to WT. Two-way ANOVA showed an increase in the volume of weak NeuN-ir in both 1-month and 12-month-old ARMS$^{+/-}$ mice ($P<0.05$) and the 12-month-old mice had a larger extent of weak NeuN-ir ($P<0.05$).

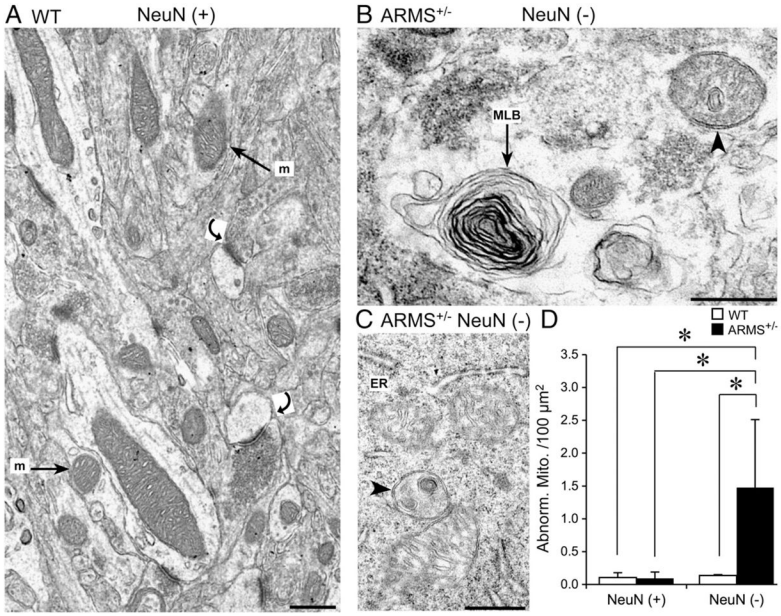

Fig. 5.

Ultrastructural evidence for mitochondrial abnormalities in ARMS$^{+/-}$ mice with weak NeuN-ir. (A) An area of the EC of a WT mouse with normal NeuN-ir (NeuN (+)) shows normal mitochondria (m; arrows). Synapses that appear normal are marked by curved arrows. (B and C) The nuclear cytoplasm from a cell in the EC of an ARMS$^{+/-}$ mouse with weak NeuN-ir (NeuN (−)), illustrates abnormal mitochondria (arrowheads) and MLBs (arrow). ER = endoplasmic reticulum. (D) There were more abnormal mitochondria in NeuN (−) areas of ARMS$^{+/-}$ mice compared to WT mice. Asterisks indicate statistical significance (P<0.05; for statistics see text). Calibration=500 nm.

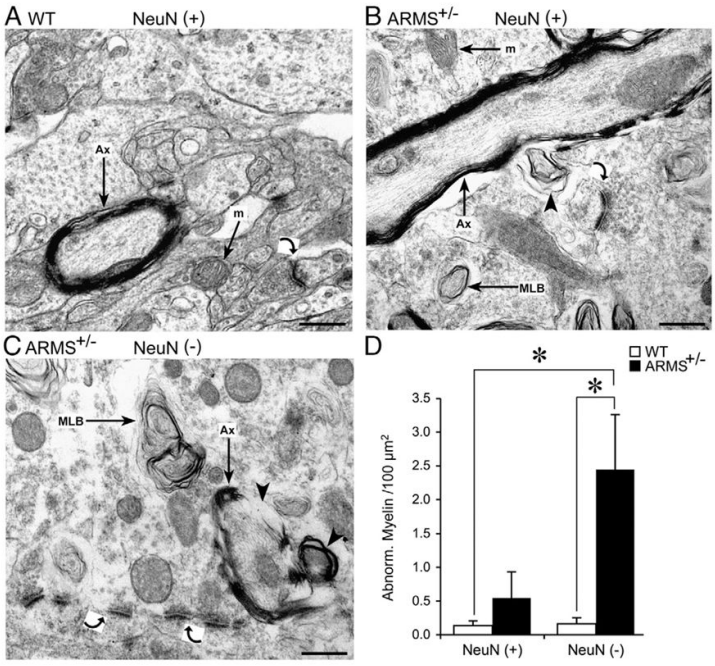

Fig. 6.

Ultrastructural evidence for abnormalities of myelination and synaptic densities in ARMS$^{+/-}$ mice. (A) In the EC of a WT mouse with normal NeuN-ir, a normal myelinated axon (Ax) and mitochondria (m) are marked by arrows. In addition, there is a synapse (curved arrow) that appears to be a normal asymmetric synapse, because there is a thickened postsynaptic density and the axon terminal contains spherical vesicles (Peters et al., 1991). (B) A longitudinal section of a myelinated axon (Ax; arrow) from a NeuN (+) area of an ARMS$^{+/-}$ mouse. An arrowhead marks a myelin whorl. (C) In an area of weak NeuN-ir (NeuN (−)) from an ARMS$^{+/-}$ mouse, a myelinated axon appears to have breaks in myelin and a myelin whorl (arrowheads). In the same area, asymmetric postsynaptic densities (curved arrows) appear to be abnormal because they are disconnected from a plasma membrane. In contrast, asymmetric postsynaptic densities in WT mice were connected to plasma membranes (see curved arrow in part A). (D) There were more abnormal myelin profiles in ARMS$^{+/-}$ mice compared to WT mice, whether NeuN (−) areas or NeuN (+) areas were examined. Asterisks indicate statistical significance ($P<0.05$; for statistics, see text). Calibration=500 nm.

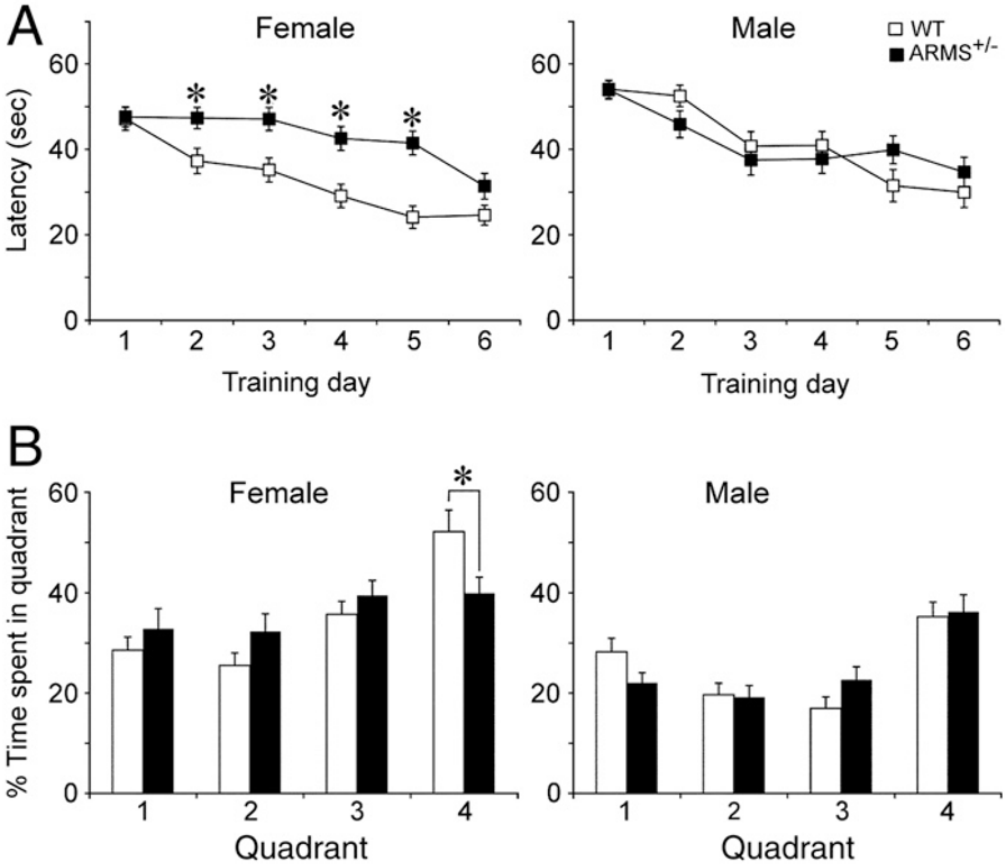

Fig. 7.

Impaired Morris water maze performance in female ARMS$^{+/-}$ mice. (A) The mean latency to find the hidden platform is shown for all days of training. Female ARMS$^{+/-}$ mice showed impairments during training compared to female WT mice. Male ARMS$^{+/-}$ mice (black) showed no significant impairments compared to male WT mice (white). Single asterisks reflect $P<0.05$ (for statistics, see text). (B) After training, animals were tested for memory of the location of the hidden platform (quadrant 4). Female ARMS$^{+/-}$ mice showed impaired performance compared to WT mice (i.e. female ARMS$^{+/-}$ mice spent less time in quadrant 4; asterisk reflects $P<0.05$). There was no impairment in memory in male mice (i.e., all animals spent more time in quadrant 4).

Table 1

Lack of brain and ventricular volume reduction in ARMS$^{+/-}$ mice.

	Total volume (mm^3)	Ventricle volume (mm^3)
Male		
WT (n=4)	255.78±12.34	5.94±0.35
ARMS$^{+/-}$ (n=4)	225.73±14.18	5.09±0.73
P	0.162	0.351
Female		
WT (n=6)	186.02±23.24	6.20±1.40
ARMS$^{+/-}$ (n=5)	225.75±20.21	6.65±0.70
P	0.229	0.780
Pooled		
WT (n=10)	213.93±18.17	6.09±0.82
ARMS$^{+/-}$ (n=9)	225.74±12.12	5.96±0.55
P	0.601	0.891

Total brain volume and ventricular volume of WT and ARMS$^{+/-}$ mice is shown. Data were generated from 3-D reconstructions of WT and ARMS$^{+/-}$ mice. There were no statistically-significant differences in total brain or ventricular volumes (Student's *t*-tests).